Earth-Based Ranging Measurements to a Planetary Radio Beacon: An Approximate Analytic Formulation

J. A. Estefan, S. W. Thurman, and M. P. Batchelder
Navigation Systems Section

An approximate analytic formulation of Earth-based ranging measurements to a radio beacon on the surface of another planet is presented. Simple mathematical models that describe lander/beacon ranging measurements are derived. Also included in this article are the partial derivatives of the range observable with respect to body-fixed coordinates of a radio beacon on the surface of a target planet. Additionally, partial derivatives are derived for target planet orientation, rotation, and for the ephemeris. View period calculations are presented for the three Deep Space Network (DSN) complexes at Goldstone, California, Canberra, Australia, and Madrid, Spain. The calculations indicate that for the case of Mars itself, total hours of visibility vary from ~280 to ~460 hours per month over a single martian synodic period (about 26 months in length), while total hours of visibility for three hypothetical beacons located along the martian prime meridian vary from ~90 to ~280 hours per month over the same period of time. Variations of the partial derivatives over time suggest that the information content of the range data is void of any singular geometries that would lead to an "ill-conditioned" information array. The only parameter that may be poorly determined, as confirmed by Viking lander range data, is the body-fixed z-height component of the surface radio beacon. The ranging model and its partial derivatives provide a sufficient framework with which to perform analytic and numerical error covariance studies of beacon location and planetary pole orientation/ephemeris determination.

I. Introduction

As part of the conceptual architectures that are currently being investigated by the National Aeronautics and Space Administration (NASA) and other, international space agencies for the exploration of Mars, it has been suggested[1] that a network of radio beacons, carried by landed and orbiting spacecraft, be deployed on the surface of the planet and in its vicinity [1]. These radio beacons could be used in a variety of applications: as spacecraft navigation aids and communications relays, for improvement of the ephemeris and determination of the polar and rotational motions of Mars, and for a number of scientific investigations in areas such as relativity experiments and studies of the geodynamics and internal structure of Mars. In the more distant future, lander and orbiter missions to other planets, their natural satellites, and asteroids may also carry radio beacons for similar purposes.

[1] R. A. Preston, R. W. Hellings, and J. B. Blamont, "A Radio Beacon on the Surface of Mars," JPL Draft Interoffice Memorandum (internal document), Jet Propulsion Laboratory, Pasadena, California, September 8, 1989.

One of the most important factors affecting the accuracy of radio metric measurements between a radio beacon and a spacecraft or Earth-based tracking stations is the level of accuracy to which the location of the beacon is known. In the case of a beacon located on the surface of another body, the utility of the beacon as a spacecraft navigation aid is limited primarily by the uncertainty in knowledge of the beacon's body-fixed location and the orientation and motion of the body with respect to inertial space, just as Earth-based radio navigation accuracy is limited by station location errors and Earth orientation errors. Range is a powerful data type for determining this information, as demonstrated by the knowledge of the ephemeris and dynamics of Mars obtained from Viking lander ranging data [2,3]. Using an S-band (2.3-GHz) range system with an accuracy of 7 m, the locations of the two Viking landers were determined with only about 6 months of Earth-based ranging data to an accuracy of $\sim$ 80 m, and the polar orientation and rotation period of Mars were determined to accuracies of $\sim$ 0.003 deg and 0.002 sec, respectively. Radio beacon designs with the capability to support an X-band (8.4-GHz) range transponder may deliver ranging accuracies to $\sim$ 1 m or better, which can yield proportionally greater lander location accuracies over the results given above for the Viking data.[2]

Although Earth-to-lander/beacon range data have been used in the past, there is generally a lack of literature describing the mathematical formulation of Earth-to-lander range measurements and the partial derivatives (information content) of this data type with respect to lander body-fixed coordinates and parameters describing the ephemeris, polar orientation, and rotation of the body on which the lander is located. As an aid to lander location and planetary ephemeris/dynamics estimation accuracy studies, this article documents an approximate analytic Earth-station-to-planetary-radio-beacon range observable formulation. In addition to a description of the general range observable and its parameter partial derivatives, the view periods of three hypothetical radio beacons located at latitudes of -45, 0, and $+45$ deg on the surface of Mars (along the prime meridian), as seen from the three Deep Space Network (DSN) sites in Goldstone, Canberra, and Madrid, are illustrated to show the total amount of potential tracking time available to the DSN over a single martian synodic period, which is about 26 months. Time histories of the associated partial derivatives at representative "snapshots" of viewing opportunities are profiled in an effort to uncover any tracking singularities that might exist.

[2] Ibid.

II. Observable Formulation

In this section, a first-order observable model for Earth-based ranging to a planetary radio beacon is derived. The model will lend itself to further development of the partial derivatives (partials) with respect to a specific set of governing parameters. Some of the notation regarding reference frames may be unfamiliar to the reader, in which case a review of the Appendix is encouraged.

A. Approximation Assumptions

Consider the geometric illustration in Fig. 1, which is fundamental to the derivation of the range observable. The vector relationship for ranging to the beacon is given by

$$\boldsymbol{\rho}^i = \mathbf{r}^i_{ET} + \mathbf{r}^i_B - \mathbf{r}^i_{sta} \tag{1}$$

where

$\mathbf{r}^i_{ET}$ = the position vector from Earth mass center to the target planet mass center

$\mathbf{r}^i_B$ = the position vector from the target planet mass center to the surface radio beacon

$\mathbf{r}^i_{sta}$ = the position vector from Earth mass center to the tracking station

The superscripts suggest that a suitable reference frame must be considered in order to derive a scalar representation of the observable. In this case, the superscript i denotes that the above vectors are expressed in Earth-centered inertial (ECI) coordinates.

To formulate the observable, consider the inner product of $\boldsymbol{\rho}^i$ with itself:

$$\begin{aligned}
\rho^2 &= \langle \boldsymbol{\rho}^i, \boldsymbol{\rho}^i \rangle \\
&= \left(\mathbf{r}^i_{ET} + \mathbf{r}^i_B - \mathbf{r}^i_{sta}\right) \cdot \left(\mathbf{r}^i_{ET} + \mathbf{r}^i_B - \mathbf{r}^i_{sta}\right) \\
&= r^2_{ET} + 2\mathbf{r}^i_{ET} \cdot \mathbf{r}^i_B - 2\mathbf{r}^i_{ET} \cdot \mathbf{r}^i_{sta} \\
&\quad + r^2_B - 2\mathbf{r}^i_B \cdot \mathbf{r}^i_{sta} + r^2_{sta}
\end{aligned}$$

which can be factored as

$$\rho^2 = r^2_{ET}\left[1 + \frac{2}{r_{ET}}\left(\frac{\mathbf{r}^i_{ET}}{r_{ET}}\right) \cdot \mathbf{r}^i_B - \frac{2}{r_{ET}}\left(\frac{\mathbf{r}^i_{ET}}{r_{ET}}\right) \cdot \mathbf{r}^i_{sta} + \frac{r^2_B}{r^2_{ET}} - \frac{2}{r^2_{ET}}(\mathbf{r}^i_B \cdot \mathbf{r}^i_{sta}) + \frac{r^2_{sta}}{r^2_{ET}}\right] \tag{2}$$

For typical magnitudes of r_{ET}, r_B, and r_{sta}, an accurate approximation for range can be obtained by neglecting the small, dimensionless quantities of order

$$\left(\frac{r_p}{r_{ET}}\right)^2$$

where

$$r_{sta} \sim r_B \sim r_p \text{ (planet radius)}$$

Using this fact, while retaining only the linear terms in a Taylor-series expansion about $\rho = (\xi + \delta\xi)^{\frac{1}{2}}$ in which

$$\xi \equiv 1 \quad \text{and} \quad \delta\xi = \frac{2}{r_{ET}}\left(\frac{\mathbf{r}^i_{ET}}{r_{ET}}\right) \cdot \left(\mathbf{r}^i_B - \mathbf{r}^i_{sta}\right)$$

Eq. (2) then reduces to

$$\rho \approx r_{ET}\left[1 + \frac{1}{r_{ET}}\left(\frac{\mathbf{r}^i_{ET}}{r_{ET}}\right) \cdot \left(\mathbf{r}^i_B - \mathbf{r}^i_{sta}\right)\right] \tag{3}$$

or simply

$$\rho = r_{ET} + \left(\frac{\mathbf{r}^i_{ET}}{r_{ET}}\right) \cdot \left(\mathbf{r}^i_B - \mathbf{r}^i_{sta}\right) \tag{4}$$

Equality is used with the understanding that this is a first-order approximation.

To complete the formulation, each term in the above relationship must be expanded into its scalar components.

B. Expanding Earth-to-Target-Planet Range

The vector $\mathbf{r}^s_{ET}$ (i.e., the position vector from Earth mass center to the target planet mass center) is expressed in plane-of-sky (POS) coordinates or s-frame of reference, and is given by (see Fig. 2)

$$\mathbf{r}^s_{ET} = [V_N \Delta t \cos\theta,\ V_N \Delta t \sin\theta,\ r_{ET_0} + V_R \Delta t\,]^{\mathrm{T}}$$

where

V_N = the velocity component of the target planet relative to Earth, lying in the plane of the sky (cross-velocity) at some epoch time $t = t_0$

V_R = the velocity component of the target planet relative to Earth, lying along the line of sight (radial velocity) at $t = t_0$

r_{ET_0} = the distance along the line of sight between Earth mass center and the target planet mass center at $t = t_0$

Δt = $(t - t_0)$, the elapsed time from the referenced epoch

θ = the angle between the cross-velocity and the X_s axis

The scalar Earth-to-target-planet range r_{ET} can be derived by employing the same approximations used to arrive at Eq. (4). Hence

$$r_{ET} \approx r_{ET_0}\left[1 + \frac{V_R}{r_{ET_0}}\Delta t\right] \tag{5}$$

or, to first-order

$$r_{ET} = r_{ET_0} + V_R \Delta t \tag{6}$$

Observe from Eq. (4) that $(\mathbf{r}^i_{ET}/r_{ET})$ is simply a *unit vector* in the direction of the target planet mass center and its i-frame components are given by (see Fig. 1)

$$\hat{\mathbf{r}}^i_{ET} \equiv \left(\frac{\mathbf{r}^i_{ET}}{r_{ET}}\right) = (\cos\delta\cos\alpha, \cos\delta\sin\alpha, \sin\delta)^{\mathrm{T}} \tag{7}$$

where

δ = the target planet declination

α = the target planet right ascension

Final steps in formulating the observable model require the expansion of $(\hat{\mathbf{r}}^i_{ET} \cdot \mathbf{r}^i_B)$ and $(\hat{\mathbf{r}}^i_{ET} \cdot \mathbf{r}^i_{sta})$. The former expression is not immediately obvious and will require further development. The latter expression, however, can be evaluated immediately, based on familiar results.

C. Inner-Product Expansion (Tracking Station)

Coordinate representation of the tracking station position vector relative to the i-frame of reference[3] is shown from Fig. 3 to be

$$\mathbf{r}^i_{sta} = \left[r^{sta}_s \cos\alpha_{sta}, r^{sta}_s \sin\alpha_{sta}, z^{sta}_h\right]^{\mathrm{T}} \tag{8}$$

where

[3] Components of the transformation from the Earth-fixed to the inertial frame due to polar motion, precession, nutation, and Earth tidal motion are ignored.

r_s^{sta} = the tracking station spin radius

$\alpha_{sta} = \theta_{g_0} + \omega_E(t - t_0) + \lambda_e^{sta}$, station right ascension

θ_{g_0} = Greenwich mean sidereal time

ω_E = Earth angular rotation rate

λ_e^{sta} = the tracking station east longitude

z_h^{sta} = the tracking station z-height

Therefore

$$\begin{aligned}(\hat{\mathbf{r}}_{ET}^{i} \cdot \mathbf{r}_{sta}^{i}) &= r_s^{sta} \cos\delta \cos\alpha \cos\alpha_{sta} \\ &\quad + r_s^{sta} \cos\delta \sin\alpha \sin\alpha_{sta} + z_h^{sta} \sin\delta \\ &= r_s^{sta} \cos\delta \,(\cos\alpha \cos\alpha_{sta} + \sin\alpha \sin\alpha_{sta}) \\ &\quad + z_h^{sta} \sin\delta\end{aligned}$$

which implies

$$(\hat{\mathbf{r}}_{ET}^{i} \cdot \mathbf{r}_{sta}^{i}) = r_s^{sta} \cos\delta \cos HA + z_h^{sta} \sin\delta \qquad (9)$$

where HA is the hour angle, defined as $HA \triangleq \alpha_{sta} - \alpha$.

D. Inner-Product Expansion (Radio Beacon)

In evaluating $(\hat{\mathbf{r}}_{ET}^{i} \cdot \mathbf{r}_{B}^{i})$, note that the difficulty arises in the fact that $\mathbf{r}_B^i$ is expressed in i-frame coordinates, a rather obscure vector quantity, at least to this point. However, an expression relative to the p-frame of reference follows immediately, and once a transformation matrix is derived that will transform this p-frame vector to its i-frame counterpart, expansion of $(\hat{\mathbf{r}}_{ET}^{i} \cdot \mathbf{r}_{B}^{i})$ can readily be performed.

The radio beacon position vector relative to the p-frame of reference (shown in Fig. 4) is given by

$$\mathbf{r}_B^p = \left[r_s^B \cos\lambda_e^B, r_s^B \sin\lambda_e^B, z_h^B\right]^{\mathrm{T}} \qquad (10)$$

where

r_s^B = the radio beacon spin radius

λ_e^B = the radio beacon east longitude

z_h^B = the radio beacon z-height

A digression is now made in order to obtain the direction cosine matrix that will transform this p-frame vector to the i-frame of reference.

Figure 5 provides a reference-frame geometry in which such a transformation matrix can be derived [4,5]. The direction of the target planet's north pole is specified by the value of its right ascension α_0 and declination δ_0. The location of the prime meridian is specified by the angle W, measured in an easterly direction along the planet's equator from point Q to point B, where the prime meridian crosses the equator. Note that the point Q is located at right ascension $(90° + \alpha_0)$ of the target planet's equator, which resides on the standard Earth equator. The inclination of the target planet's equator to the standard Earth equator is $(90° - \delta_0)$.

The angles α_0, δ_0, and W are assumed to vary linearly with time and are implicitly expressed as $\alpha_0 = \alpha_{0_0} + \dot{\alpha_0}T$, $\delta_0 = \delta_{0_0} + \dot{\delta_0}T$, and $W = W_0 + W_1 d$, where W_1 is the angular rotation rate of the target planet. The term T is the interval in Julian centuries (of 36,525 days) from some standard epoch, while d is the interval in days from the chosen standard epoch. Each can be expressed as

$$d = \text{J.D.}_{(\text{obs})} - \text{J.D.}_{(0)} \qquad (11)$$

and

$$T = \frac{d}{36{,}525} \qquad (12)$$

where $\text{J.D.}_{(\text{obs})}$ is the Julian date of the time of observation, and $\text{J.D.}_{(0)}$ is the Julian date of the standard epoch (e.g., 2451545.0).[4]

If the orthogonal triad of i-frame axes X_i, Y_i, and Z_i, as well as the orthogonal triad of p-frame axes X_p, Y_p, and Z_p, are hypothetically superimposed on Fig. 5 such that all the axes are oriented as they are defined in the Appendix, then the transformation matrix from the p-frame to the i-frame can be computed via three successive rotations. A positive rotation about the Z_i axis through the angle $(90° + \alpha_0)$ will align the X_i axis with the point Q. This is represented by the orthogonal rotation matrix

$$\mathbf{R}_3(90° + \alpha_0) = \begin{bmatrix} -\sin\alpha_0 & \cos\alpha_0 & 0 \\ -\cos\alpha_0 & -\sin\alpha_0 & 0 \\ 0 & 0 & 1 \end{bmatrix}$$

Next, a positive rotation about the resultant X_i axis through the angle $(90° - \delta_0)$ will align the standard Earth equator with the target planet's equator. This is represented by the orthogonal rotation matrix

[4] Again, the standard epoch used here is J2000.0.

$$\mathbf{R}_1(90^\circ - \delta_0) = \begin{bmatrix} 1 & 0 & 0 \\ 0 & \sin\delta_0 & \cos\delta_0 \\ 0 & -\cos\delta_0 & \sin\delta_0 \end{bmatrix}$$

Finally, a positive rotation about the resultant Z_i axis through the angle W will align the **i**-frame axes with the **p**-frame axes at the target planet prime meridian. This is represented by the orthogonal rotation matrix

$$\mathbf{R}_3(W) = \begin{bmatrix} \cos W & \sin W & 0 \\ -\sin W & \cos W & 0 \\ 0 & 0 & 1 \end{bmatrix}$$

The direction cosine matrix that transforms vectors expressed in the **i**-frame to vectors expressed in the **p**-frame is then given by

$$\mathbf{R}_i^p \equiv \mathbf{R}_3(W)\,\mathbf{R}_1(90^\circ - \delta_0)\,\mathbf{R}_3(90^\circ + \alpha_0) \tag{13}$$

Note, however, that the desired transformation matrix is $\mathbf{R}_p^i$, but because $\mathbf{R}_i^p$ is orthogonal

$$\mathbf{R}_p^i = (\mathbf{R}_i^p)^{\mathrm{T}} \tag{14}$$

Carrying out the above matrix computations

$$\mathbf{R}_p^i = \begin{bmatrix} \mathrm{R}_{11} & \mathrm{R}_{12} & \mathrm{R}_{13} \\ \mathrm{R}_{21} & \mathrm{R}_{22} & \mathrm{R}_{23} \\ \mathrm{R}_{31} & \mathrm{R}_{32} & \mathrm{R}_{33} \end{bmatrix} \tag{15}$$

where

$$\begin{aligned}
\mathrm{R}_{11} &= -(\cos W \sin\alpha_0 + \sin W \sin\delta_0 \cos\alpha_0) \\
\mathrm{R}_{12} &= \sin W \sin\alpha_0 - \cos W \sin\delta_0 \cos\alpha_0 \\
\mathrm{R}_{13} &= \cos\delta_0 \cos\alpha_0 \\
\mathrm{R}_{21} &= \cos W \cos\alpha_0 - \sin W \sin\delta_0 \sin\alpha_0 \\
\mathrm{R}_{22} &= -(\sin W \cos\alpha_0 + \cos W \sin\delta_0 \sin\alpha_0) \\
\mathrm{R}_{23} &= \cos\delta_0 \sin\alpha_0 \\
\mathrm{R}_{31} &= \sin W \cos\delta_0 \\
\mathrm{R}_{32} &= \cos W \cos\delta_0 \\
\mathrm{R}_{33} &= \sin\delta_0
\end{aligned}$$

From this development and the fact that

$$\mathbf{r}_B^i = \mathbf{R}_p^i\,\mathbf{r}_B^p \tag{16}$$

the inner product $(\hat{\mathbf{r}}_{ET}^i \cdot \mathbf{r}_B^i)$ can finally be expanded. Hence

$$\begin{aligned}
(\hat{\mathbf{r}}_{ET}^i \cdot \mathbf{r}_B^i) = r_s^B \Big[& \cos\delta \cos\left(W + \lambda_e^B\right) \sin(\alpha - \alpha_0) \\
& - \cos\delta \sin\delta_0 \sin\left(W + \lambda_e^B\right) \cos(\alpha - \alpha_0) \\
& + \sin\delta \cos\delta_0 \sin\left(W + \lambda_e^B\right) \Big] \\
& + z_h^B \left[\cos\delta \cos\delta_0 \cos(\alpha - \alpha_0) + \sin\delta \sin\delta_0\right]
\end{aligned} \tag{17}$$

where $W + \lambda_e^B$ is the east longitude of the beacon relative to the standard Earth equator.

E. The Observable

The first-order range observable is found by substituting Eqs. (6), (9), and (17) into Eq. (4), yielding

$$\begin{aligned}
\rho = {} & r_{ET_0} + V_R \Delta t \\
& + r_s^B \Big[\cos\delta \cos\left(W + \lambda_e^B\right) \sin(\alpha - \alpha_0) \\
& - \cos\delta \sin\delta_0 \sin\left(W + \lambda_e^B\right) \cos(\alpha - \alpha_0) \\
& + \sin\delta \cos\delta_0 \sin\left(W + \lambda_e^B\right) \Big] - r_s^{sta} \cos\delta \cos HA \\
& + z_h^B \left[\cos\delta \cos\delta_0 \cos(\alpha - \alpha_0) + \sin\delta \sin\delta_0\right] - z_h^{sta} \sin\delta
\end{aligned} \tag{18}$$

It is important to note that the prime meridian is only an intermediary and arbitrarily selected meridian.

Some immediate observations can be made about the observable model as expressed above:

(1) The right ascension (α) of the target planet and its pole (α_0) appear only in those terms in the combination $\alpha - \alpha_0$.

(2) The model clearly distinguishes between the "fast terms" (i.e., the period of a day, $W + \lambda_e^B$), and the "slow terms" (all others).

(3) The right ascension (α) and declination (δ) of the target planet vary with relative planetary motion (e.g., the synodic period $\sim$ a few years).

(4) The right ascension (α_0) and declination (δ_0) of the target planet's pole vary with the precession period. (Very long, indeed!)

(5) For long-term analyses, the Earth-to-target-planet range (r_{ET}) varies in a more complex manner than the simple linear behavior depicted by $r_{ET} = r_{ET_0} + V_R \Delta t$—it also varies with terms at the synodic period.

III. Range Observable Partial Derivatives (Partials)

This section provides the partials (information content) of the range observable. Specifically, partials will be developed with respect to:

(1) the body-fixed coordinates of a surface radio beacon,

(2) the target planet pole orientation,

(3) the target planet polar motion (nutation and precession),

(4) the target planet rotation rate, and

(5) the target planet ephemeris.

The location of the prime meridian cannot be discerned independently from the lander/beacon longitude (i.e., both prime meridian and longitude errors leave identical signatures in the ranging signal); hence, its partial is omitted.

1. Beacon coordinates.

$$\left(\frac{\partial \rho}{\partial r_s^B}\right) = \cos\delta \cos\left(W + \lambda_e^B\right) \sin(\alpha - \alpha_0) - \cos\delta \sin\delta_0 \sin\left(W + \lambda_e^B\right) \cos(\alpha - \alpha_0) + \sin\delta \cos\delta_0 \sin\left(W + \lambda_e^B\right) \tag{19}$$

$$\left(\frac{\partial \rho}{\partial \lambda_e^B}\right) = -r_s^B \left[\cos\delta \sin\left(W + \lambda_e^B\right) \sin(\alpha - \alpha_0) + \cos\delta \sin\delta_0 \cos\left(W + \lambda_e^B\right) \cos(\alpha - \alpha_0) - \sin\delta \cos\delta_0 \cos\left(W + \lambda_e^B\right)\right] \tag{20}$$

$$\left(\frac{\partial \rho}{\partial z_h^B}\right) = \cos\delta \cos\delta_0 \cos(\alpha - \alpha_0) + \sin\delta \sin\delta_0 \tag{21}$$

2. Pole orientation.

$$\left(\frac{\partial \rho}{\partial \alpha_0}\right) = -r_s^B \cos\delta \left[\cos\left(W + \lambda_e^B\right) \cos(\alpha - \alpha_0) + \sin\delta_0 \sin\left(W + \lambda_e^B\right) \sin(\alpha - \alpha_0)\right] + z_h^B \cos\delta \cos\delta_0 \sin(\alpha - \alpha_0) \tag{22}$$

$$\left(\frac{\partial \rho}{\partial \delta_0}\right) = -r_s^B \left[\cos\delta \cos\delta_0 \sin\left(W + \lambda_e^B\right) \cos(\alpha - \alpha_0) + \sin\delta \sin\delta_0 \sin\left(W + \lambda_e^B\right)\right] - z_h^B \left[\cos\delta \sin\delta_0 \cos(\alpha - \alpha_0) - \sin\delta \cos\delta_0\right] \tag{23}$$

3. Polar motion. Recall that $\alpha_0 = \alpha_{0_0} + \dot{\alpha_0} T$ and $\delta_0 = \delta_{0_0} + \dot{\delta_0} T$. Hence

$$\left(\frac{\partial \rho}{\partial \dot{\alpha_0}}\right) = -r_s^B \cos\delta\, T \left[\cos\left(W + \lambda_e^B\right) \cos(\alpha - \alpha_0) + \sin\delta_0 \sin\left(W + \lambda_e^B\right) \sin(\alpha - \alpha_0)\right] + z_h^B \cos\delta\, T \cos\delta_0 \sin(\alpha - \alpha_0) = \left(\frac{\partial \rho}{\partial \alpha_0}\right) T \tag{24}$$

$$\left(\frac{\partial \rho}{\partial \dot{\delta_0}}\right) = -r_s^B T \left[\cos\delta \cos\delta_0 \sin\left(W + \lambda_e^B\right) \cos(\alpha - \alpha_0) + \sin\delta \sin\delta_0 \sin\left(W + \lambda_e^B\right)\right] - z_h^B T \left[\cos\delta \sin\delta_0 \cos(\alpha - \alpha_0) - \sin\delta \cos\delta_0\right] = \left(\frac{\partial \rho}{\partial \delta_0}\right) T \tag{25}$$

4. Rotation rate. Recall that $W = W_0 + W_1 d$, which implies $(W + \lambda_e^B) = W_0 + \lambda_e^B + W_1 d$. Hence

$$\left(\frac{\partial \rho}{\partial W_1}\right) = -r_s^B d\Big[\cos\delta \sin\left(W + \lambda_e^B\right) \sin(\alpha - \alpha_0)$$

$$+ \cos\delta \sin\delta_0 \cos\left(W + \lambda_e^B\right) \cos(\alpha - \alpha_0)$$

$$- \sin\delta \cos\delta_0 \cos\left(W + \lambda_e^B\right)\Big]$$

$$= \left(\frac{\partial \rho}{\partial \lambda_e^B}\right) d \tag{26}$$

5. **Ephemeris.**

$$\left(\frac{\partial \rho}{\partial r_{ET_0}}\right) = 1 \tag{27}$$

$$\left(\frac{\partial \rho}{\partial \alpha}\right) = r_s^B \Big[\cos\delta \cos\left(W + \lambda_e^B\right) \cos(\alpha - \alpha_0)$$

$$+ \cos\delta \sin\delta_0 \sin\left(W + \lambda_e^B\right) \sin(\alpha - \alpha_0)\Big]$$

$$- r_s^{sta} \cos\delta \sin HA$$

$$- z_h^B \cos\delta \cos\delta_0 \sin(\alpha - \alpha_0) \tag{28}$$

$$\left(\frac{\partial \rho}{\partial \delta}\right) = -r_s^B \Big[\sin\delta \cos\left(W + \lambda_e^B\right) \sin(\alpha - \alpha_0)$$

$$- \sin\delta \sin\delta_0 \sin\left(W + \lambda_e^B\right) \cos(\alpha - \alpha_0)$$

$$- \cos\delta \cos\delta_0 \sin\left(W + \lambda_e^B\right)\Big]$$

$$+ r_s^{sta} \sin\delta \cos HA$$

$$- z_h^B \left[\sin\delta \cos\delta_0 \cos(\alpha - \alpha_0) - \cos\delta \sin\delta_0\right]$$

$$- z_h^{sta} \cos\delta \tag{29}$$

IV. Analysis

This article does not present any results based on error covariance analyses; however, a brief investigation of the information content of Earth-to-beacon range data is performed in which the time behavior of the partials is scrutinized to uncover potential geometric singularities[5] that might exist—certainly, useful knowledge prior to beginning error covariance studies. Until now, the focus has been on the general case of Earth-based ranging to a radio beacon on the surface of any terrestrial target planet; in this section, attention is restricted to a radio beacon on the surface of Mars.

A. Observation Schedules (View Periods)

Two software tools developed at the Jet Propulsion Laboratory (JPL) are used for view period computations:

(1) a computer program entitled *DSN Plan*, which can compute Mars view periods for a specified set of DSN stations,[6] and

(2) a computer program entitled *Planetary Observer Planning Software (POPS)*, which can compute a set of view periods for the more constrained case of a surface radio beacon for a specified set of DSN stations.[7]

Figure 6 indicates the total amount of visibility in hours for Mars over the course of a representative 26-month period (January 1, 1995 through February 28, 1997, or a little over one martian synodic period) for each of the DSN complexes (Goldstone, Canberra, and Madrid[8]). The actual daily observation schedules are omitted for brevity. Figure 7 indicates the total amount of visibility in hours for a radio beacon on the surface of Mars located *on* the equator *at* the prime meridian for each of the DSN sites. The trends are similar to those shown in Fig. 6 for the planet-tracking case, but with about a factor of two reduction in total hours of visibility. Figures 8 and 9 profile the total amount of visibility in hours for beacons located at +45 deg and −45 deg (i.e., 45° N and 45° S) areocentric latitudes, respectively, along the prime meridian. The reduction in total hours of visibility compared with the planet-tracking case is also about a factor of two; yet the trends are quite different from the equatorial-beacon case of Fig. 7. For the +45-deg site, the northern and southern

[5] Regions where a given partial derivative may have near-zero magnitude.

[6] S. L. Van Dillen, *DSN Plan User's Guide*, EM 93-269 (internal document), Jet Propulsion Laboratory, Pasadena, California, July 25, 1975.

[7] J. Smith, "Planetary Observer Planning Software (POPS) Version 2.0," viewgraph presentation (internal document), Mission Design Section, Jet Propulsion Laboratory, Pasadena, California, May 31, 1990.

[8] The corresponding Deep Space Communications Complexes (DSCCs) at these locations are labeled in the figure as DSCC 10, DSCC 40, and DSCC 60, respectively.

hemisphere complexes maintain a similar behavior over the course of the synodic period with a few minor digressions in individual trends, while the −45-deg case demonstrates a slightly greater shift in total hours of visibility between the northern and southern hemisphere complexes.

B. Time History of the Partials

In order to assess the time behavior of the partials, a single pass of beacon tracking data is assumed to be collected for each of four days that span the selected observation year, which is taken to be 1995. These particular days are selected arbitrarily near the beginning of each quarter, and no attempt is made to identify those that would optimize tracking coverage in terms of maximum available viewing time. The schedule is shown in Table 1 and illustrates four representative "snapshots" of viewing opportunities over the course of the 1995 calendar year. The table also shows the associated martian ephemeris data that were obtained from JPL planetary ephemerides [6].

Time histories (variations) of the partials with respect to body-fixed coordinates, pole orientation, polar motion, and angular rotation rate for a radio beacon located on the equator at the prime meridian are shown in Figs. 10 through 13, with viewing times rounded to the nearest quarter hour. (Variations of the ephemeris partials are omitted for brevity.)

Figure 10(a) profiles the variation of the partial with respect to the spin radius of the radio beacon; no singular regions are seen to exist. Figure 10(b) shows the variation of the associated east longitude partial, which is also void of any near singularity regions; Fig. 10(c) illustrates the variation of the z-height partial. In this case, the time histories have a linear behavior—a rather unfortunate result since, over time, the data arc will eventually drift so that this partial may be nearly zero (no information content) for significant periods of time. This phenomenon, of course, agrees with the familiar notion that line-of-sight data types such as range have difficulty in determining the body-fixed z-height direction and are frequently absorbed into an ephemeris error [2].

Figure 11(a) profiles the variation of the partial of the range observable with respect to right ascension of the pole for each of the selected days of observation. The data are assumed to be collected from DSCC 10 (Goldstone) for this parameter as well as for all other parameters described herein. No singular (near-zero) regions are seen to exist in this case. Figure 11(b) shows the variation of the associated declination partial. The data contain a good signature avoiding the singular regions for the duration of each observation.

Figure 12(a) illustrates the variation of the partial with respect to the right ascension rate of the pole, and suggests that the information content of the data is substantial in this case. (The units of JC represent Julian centuries.) Figure 12(b) shows the variation of the associated declination rate partial: a good signature is maintained, and similar to Fig. 11(b), near-zero regions are avoided.

Figure 13 shows the variation of the partial with respect to the Mars angular rotation rate. The information content of the data appears to be substantial and void of near-zero regions.

V. Conclusions

An approximate analytic model for Earth-based ranging to a planetary radio beacon was formulated. The model for the observable was shown to lend itself to a simple derivation of the partial derivatives (information content) of the data. The resulting analytic expressions are intended to aid in lander/beacon location and planetary ephemeris/dynamics estimation accuracy studies and can easily be mechanized into related software tools. View periods were computed for three hypothetical radio beacons located on the surface of Mars, as seen from the three DSN sites at Goldstone, Canberra, and Madrid, over the course of a single martian synodic period. View periods for the less constrained viewing geometry of observing the planet itself were also computed. The results helped to facilitate the construction of a representative observation schedule for use in computing time histories of the partials. Total potential tracking time available at each DSN site was seen to vary from $\sim$ 280 to $\sim$ 460 hours per month over a representative synodic period for the case of viewing the planet itself, and $\sim$ 90 to $\sim$ 280 hours per month for the cases shown in tracking hypothetical surface radio beacons at three different sites (northern and southern hemispheres and equator) along the prime meridian. In an effort to identify any parameters that potentially cannot be determined very well from range data, variations of the partials over time were shown for the location parameters of a surface radio beacon, as well as for Mars orientation and rotation parameters. The results confirm the findings of previous studies and the Viking experience, in that all associated parameters, with the possible exception of lander/beacon body-fixed z-height, can be well determined from range data.

Acknowledgment

The authors thank Jean-Paul Berthias for his technical comments and careful review of the subject matter presented in this article. His helpful suggestions and constant professionalism have proved invaluable in completing this work.

References

[1] L. Boloh, J. Y. Prado, G. Laurans, and P. Savary, Centre National d'Etudes Spatiales, Toulouse, France, "A Radio Beacon for the Exploration of Planet Mars," presented at the AIAA/JPL Second International Conference on Solar System Exploration, Pasadena, California, August 22–24, 1989.

[2] A. P. Mayo, W. T. Blackshear, R. H. Tolson, and W. H. Michael, Jr., "Lander Locations, Mars Physical Ephemeris, and Solar System Parameters: Determination From Viking Lander Tracking Data," *Journal of Geophysical Research*, vol. 82, no. 28, pp. 4297–4303, 1977.

[3] N. Borderies, G. Balmino, L. Castel, and B. Moynot, "Study of Mars Dynamics From Lander Tracking Data Analysis," *The Moon and the Planets*, vol. 22, Dordrecht, Holland and Boston, Massachusetts: D. Reidel Publishing Co., 1980.

[4] M. E. Davies, V. K. Abalakin, C. A. Cross, R. L. Duncombe, H. Masursky, B. Morando, T. C. Owen, P. K. Seidelmann, A. T. Sinclair, G. A. Wilkins, and Y. S. Tjuflin, "Report of the IAU Working Group on Cartographic Coordinates and Rotational Elements of the Planets and Satellites," *Celestial Mechanics*, vol. 22, no. 2, pp. 222–228, 1980.

[5] M. E. Davies, V. K. Abalakin, M. Burša, G. E. Hunt, J H. Lieske, B. Morando, R. H. Rapp, P. K. Seidelmann, A. T. Sinclair, and Y. S. Tjuflin, "Report of the IAU/IAG/COSPAR Working Group on Cartographic Coordinates and Rotational Elements of the Planets and Satellites: 1988," *Celestial Mechanics and Dynamical Astronomy*, vol. 46, no. 2, pp. 187–204, 1989.

[6] *Planetary and Lunar Coordinates for the Years 1984–2000*, London: Her Majesty's Stationery Office, and Washington, D. C.: U. S. Government Printing Office, ISBN 0-11-886917-5, 1983.

Table 1. Radio beacon observation schedule and the associated Mars right ascension (α), declination (δ), and distance (r_{ET})

Date	Rise time, GMT	Set time, GMT	α, deg	δ, deg	r_{ET}, AU
January 8, 1995	13:00	17:41	155.9135	+14.041	0.79805
April 8–9, 1995	20:56	30:51	137.7624	+19.250	0.95328
July 7, 1995	03:26	06:31	172.7026	+ 3.866	1.69372
October 15–16, 1995	21:00	26:49	233.4047	−19.817	2.18804

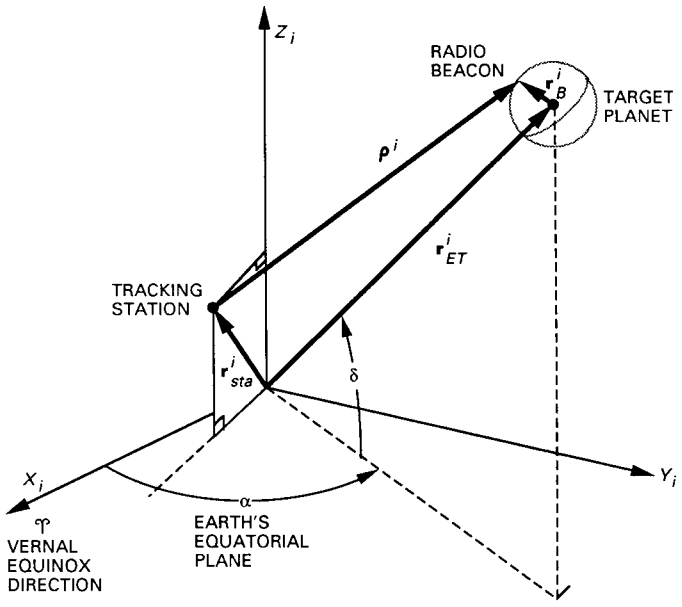

Fig. 1. Earth-to-target-planet ranging geometry.

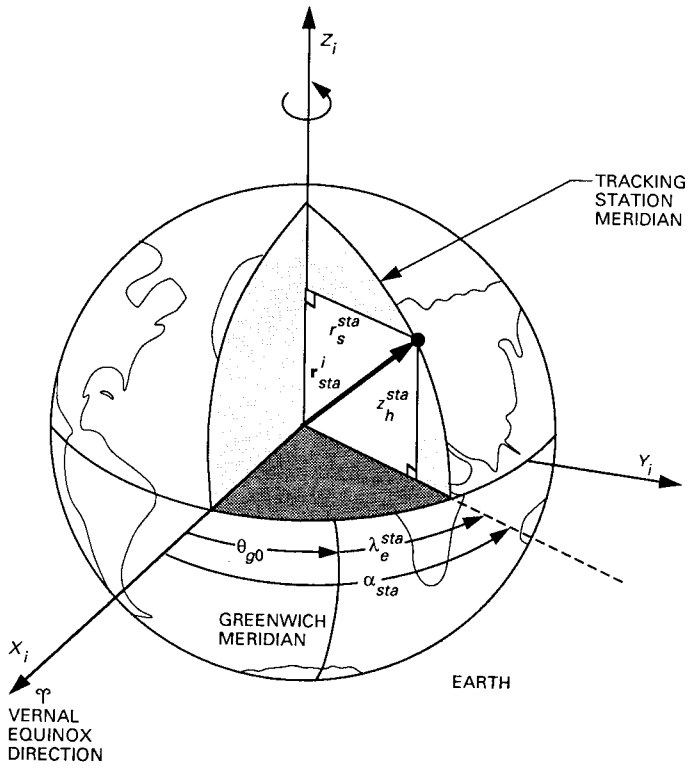

Fig. 3. Tracking station cylindrical coordinates.

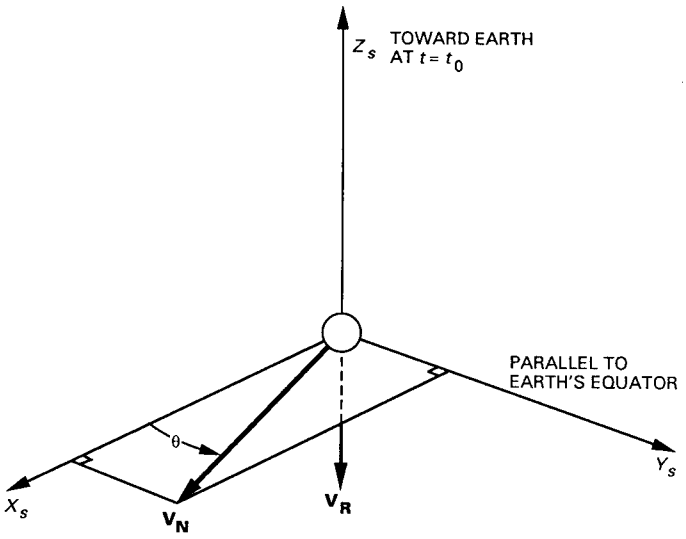

Fig. 2. Target planet orientation in the plane of the sky.

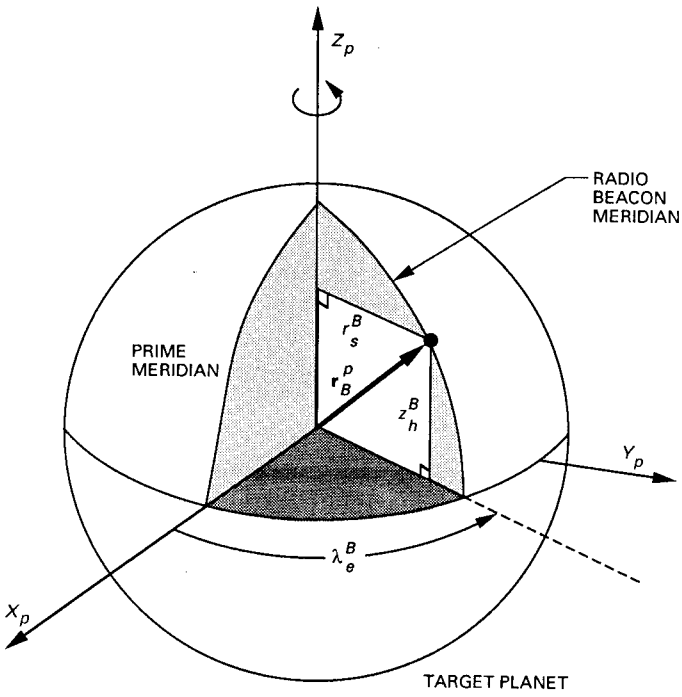

Fig. 4. Radio beacon cylindrical coordinates.

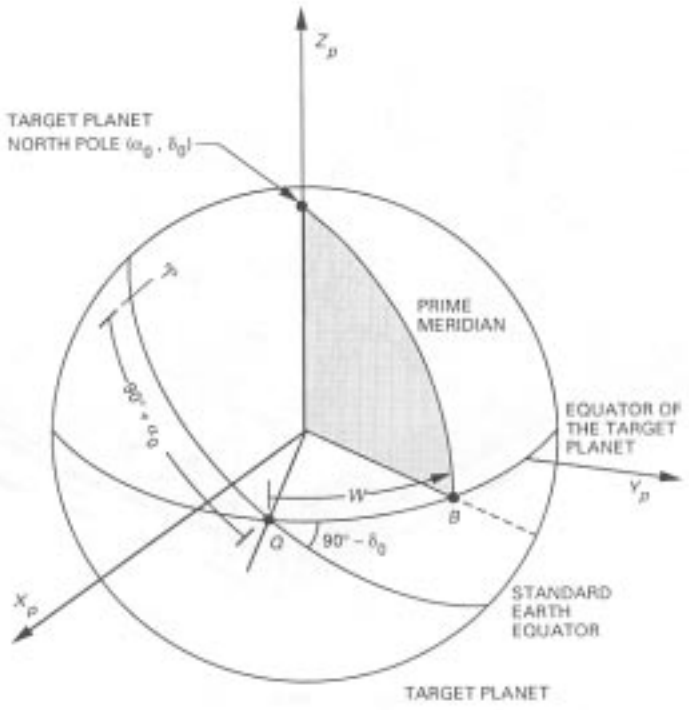

Fig. 5. Earth–target planet relative orientation.

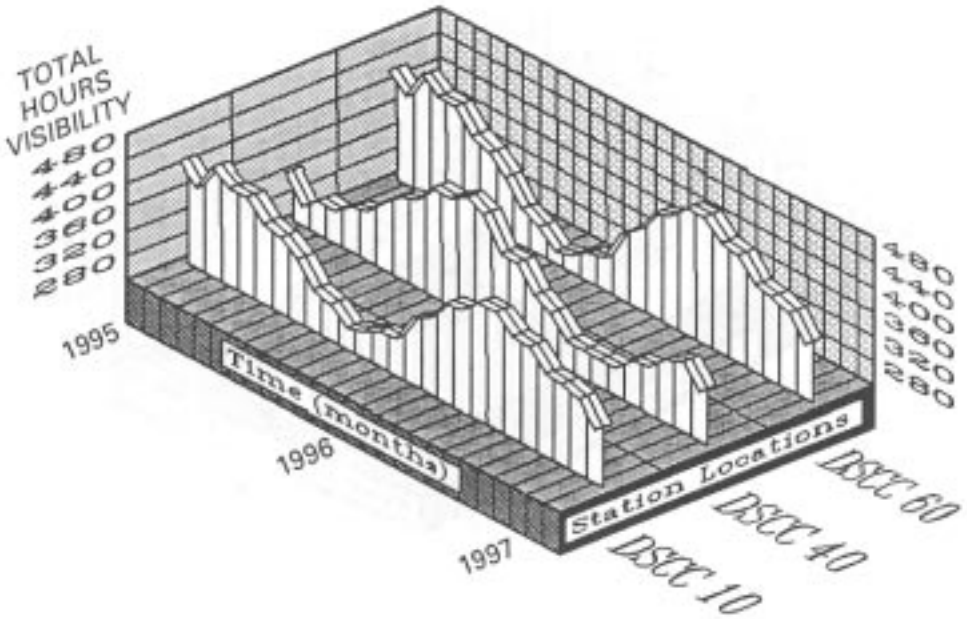

Fig. 6. Monthly visibilities of Mars from January 1, 1995–February 28, 1997 for DSN complexes DSCC 10 (Goldstone), DSCC 40 (Canberra), and DSCC 60 (Madrid).

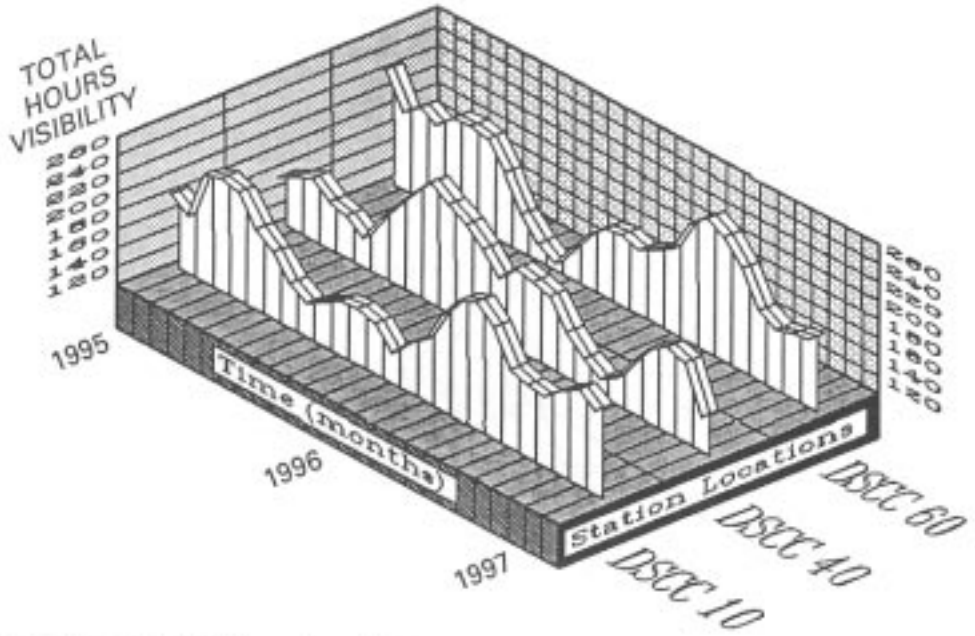

Fig. 7. Monthly visibilities of a radio beacon on Mars, located on the equator at the prime meridian, from January 1, 1995–February 28, 1997 for DSN complexes DSCC 10 (Goldstone), DSCC 40 (Canberra), and DSCC 60 (Madrid).

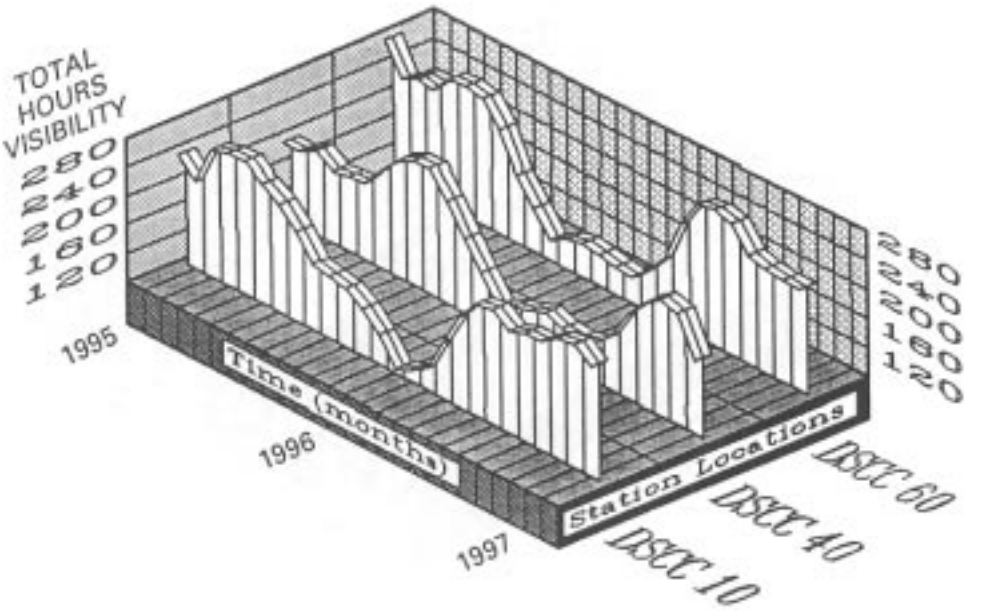

Fig. 8. Monthly visibilities of a prime meridian radio beacon at a +45-deg areocentric latitude from January 1, 1995–February 28, 1997 for DSN complexes DSCC 10 (Goldstone), DSCC 40 (Canberra), and DSCC 60 (Madrid).

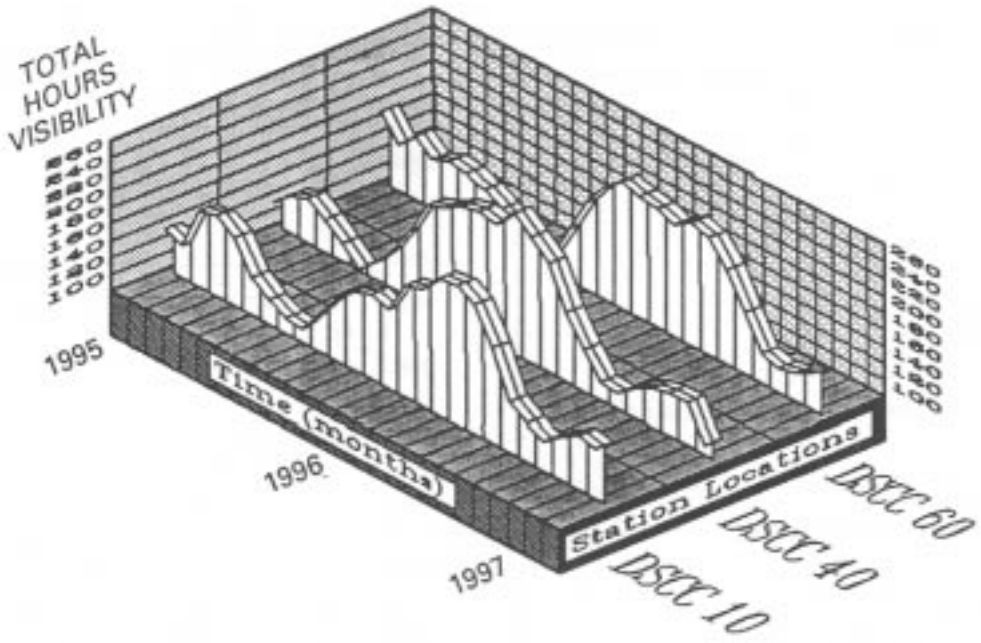

Fig. 9. Monthly visibilities of a prime meridian radio beacon at a −45-deg areocentric latitude from January 1, 1995–February 28, 1997 for DSN complexes DSCC 10 (Goldstone), DSCC 40 (Canberra), and DSCC 60 (Madrid).

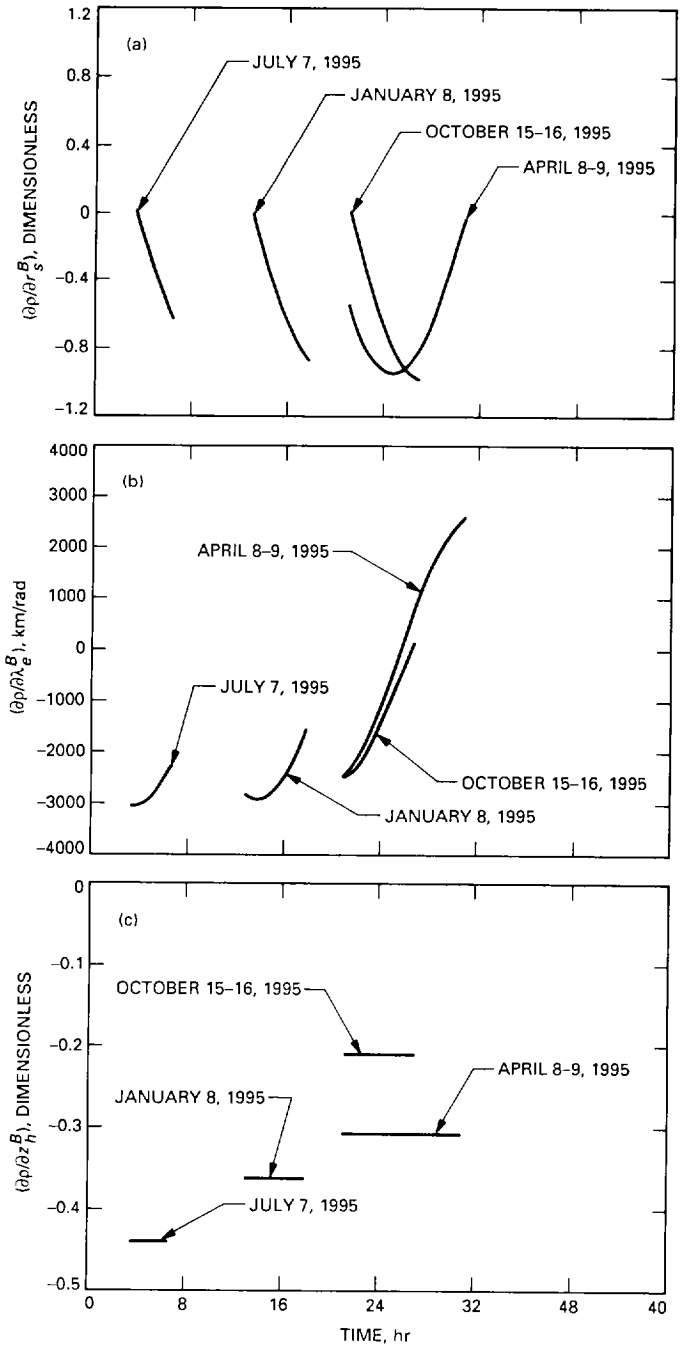

Fig. 10. Variation of the partial, versus time, with respect to: (a) the radio beacon spin radius; (b) the radio beacon east longitude; and (c) the radio beacon z-height.

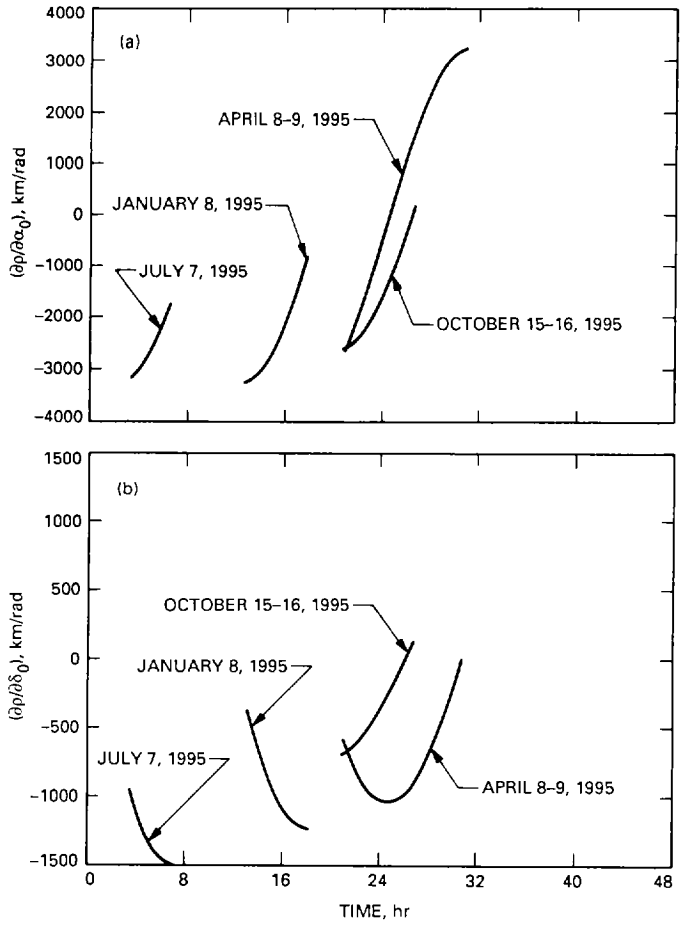

Fig. 11. Variation of the partial, versus time, with respect to: (a) the right ascension of the martian pole, and (b) the declination of the martian pole.

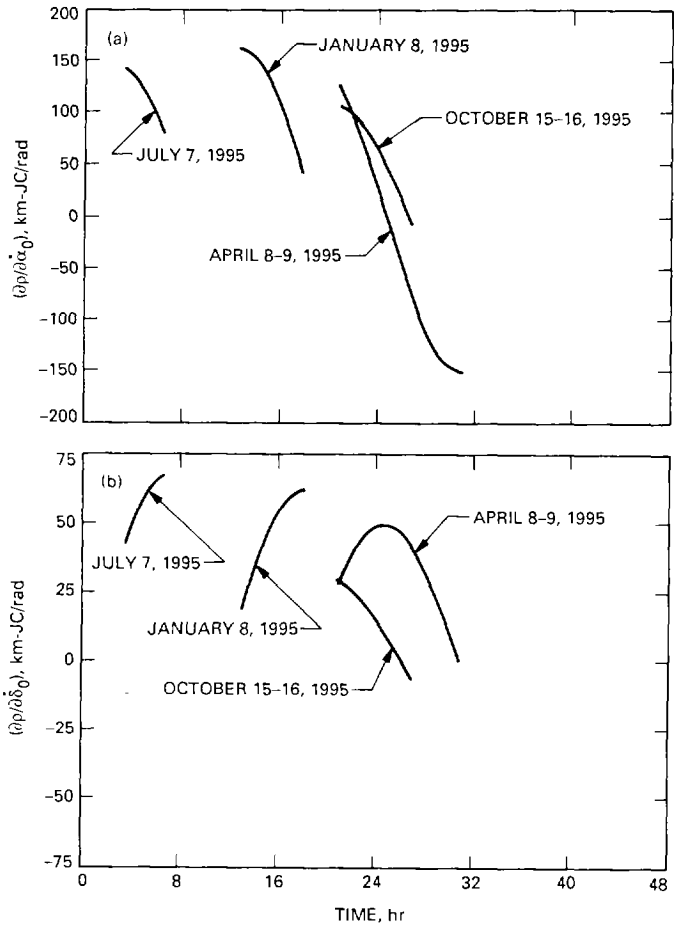

Fig. 12. Variation of the partial, versus time, with respect to: (a) the right ascension rate of the martian pole, and (b) the declination rate of the martian pole.

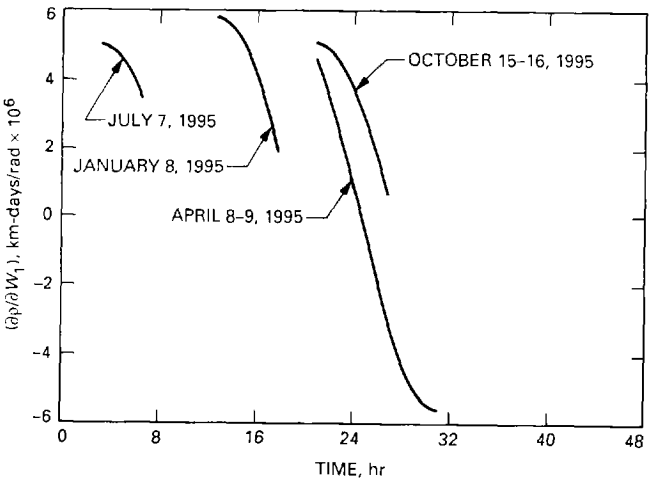

Fig. 13. Variation of the partial, versus time, with respect to the angular rotation rate of Mars.

Appendix
Definitions of Key Coordinate Frames

The following approximations are assumed:

(1) Earth and the target planet are rigid bodies.

(2) With respect to true inertial space, Earth and the target planet spin at constant rates about their axes of rotation.

A. Earth-Centered Inertial (ECI) Coordinates (i-frame)

The i-frame of reference is defined to be in alignment with the Earth mean equator and equinox of J2000.0 and is a right-handed orthogonal triad of axes X_i, Y_i, and Z_i centered at the mass center of the Earth. As shown in Fig. 1, the Z_i axis is directed through the Earth's north pole, while the X_i and Y_i axes lie in the plane of the equator. The X_i axis is directed toward the first point of Aries and the Y_i axis is directed so as to complete the right-handed system of coordinates.

B. Plane-of-Sky (POS) Coordinates (s-frame)

The s-frame of reference is defined as a right-handed orthogonal triad of axes X_s, Y_s, and Z_s centered at the target planet mass center. As shown in Fig. 2, the Z_s axis is directed toward the Earth at some epoch time, $t = t_0$, while the X_s and Y_s axes lie in the plane of the sky. The Y_s axis is directed to be parallel to the standard Earth equator and the X_s axis is directed so as to complete the right-handed system of coordinates.

C. Planet-Centered, Planet-Fixed (PCPF) Coordinates (p-frame)

The p-frame of reference is defined as a right-handed orthogonal triad of axes X_p, Y_p, and Z_p centered at the mass center of some planet. As shown in Fig. 3, the Z_p axis is directed through the planet's north pole, while the X_p and Y_p axes lie in the plane of the equator. The X_p axis is directed through the prime meridian, and the Y_p axis is directed through the 90-deg east longitude meridian.